CARDIFF UNIVERSITY
PRIFYSGOL CAERDYDD

ORCA – Online Research @ Cardiff

This is an Open Access document downloaded from ORCA, Cardiff University's institutional repository:https://orca.cardiff.ac.uk/id/eprint/114491/

This is the author's version of a work that was submitted to / accepted for publication.

Citation for final published version:

Koudouna, Elena , Mikula, Eric, Brown, Donald J., Young, Robert D. , Quantock, Andrew J. and Jester, James V. 2018. Cell regulation of collagen fibril macrostructure during corneal morphogenesis. Acta Biomaterialia 79 , pp. 96-112. 10.1016/j.actbio.2018.08.017

Publishers page: http://dx.doi.org/10.1016/j.actbio.2018.08.017

Please note:
Changes made as a result of publishing processes such as copy-editing, formatting and page numbers may not be reflected in this version. For the definitive version of this publication, please refer to the published source. You are advised to consult the publisher's version if you wish to cite this paper.

This version is being made available in accordance with publisher policies. See http://orca.cf.ac.uk/policies.html for usage policies. Copyright and moral rights for publications made available in ORCA are retained by the copyright holders.

Cell regulation of collagen fibril macrostructure during corneal morphogenesis

Running Title: Regulated assembly of collagen fibril macrostructure

Elena Koudouna[1,2], Eric Mikula[1], Donald J Brown[1], Robert D Young[2], Andrew J Quantock[2], James V Jester[1,3]

[1] Gavin Herbert Eye Institute, University of California, Irvine, Irvine, California, USA

[2] Structural Biophysics Research Group, School of Optometry and Vision Sciences, Cardiff University, Cardiff, Wales, UK

3 Department of Biomedical Engineering, University of California, Irvine, Irvine, California, USA.

Keywords: collagen, keratocytes, corneal development, cell-matrix interactions, second harmonic generation imaging

Correspondence: James V. Jester, Ph.D., 843 Health Sciences Road, University of California, Irvine, Irvine, California, USA, 92697-4390. Email: JJester@uci.edu

Support: BBSRC BB/M025349/1 (AJQ), NIH NEI EY024600 (JVJ), Research to Prevent Blindness, Inc. The Skirball Program in Molecular Ophthalmology.

Summary: Evolutionary changes in the corneal collagen structural organization, identified by second harmonic generation (SHG) microscopy are associated with the development of a refractive lens. Koudouna et al. show a convergent role for keratocytes in the organization of corneal stroma matrix.

Abstract

While tissue form and function is highly dependent upon tissue-specific collagen composition and organization, little is known of the mechanisms controlling the bundling of collagen fibrils into fibers and larger structural designs that lead to the formation of bones, tendons and other tissues. Using the cornea as a model system, our previous 3 dimensional mapping of collagen fiber organization has demonstrated that macrostructural organization of collagen fibers involving interweaving, branching and anastomosing plays a critical role in controlling mechanical stiffness, corneal shape and refractive power. In this work, the cellular and mechanical mechanisms regulating critical events in the assembly of collagen macrostructure are analysed in the developing chicken cornea. We elucidated the temporal events leading to adult corneal structure and determined the effects of intraocular pressure (IOP) on the organization of the collagen macrostructure. Our findings indicate that the complex adult collagen organization begins to appear on embryonic day 10 (E10) after deposition of the primary stroma and full invasion of keratocytes. Importantly, organizational changes in keratocytes appearing at E9 preceded and predicted later changes in collagen organization. Corneal collagen organization remained unaffected when the development of IOP was blocked at E4. These findings support a primary role for keratocytes in controlling stromal organization, mechanical stiffness and corneal shape that are not regulated by the IOP. Our findings also suggest that the avian cornea represents an excellent experimental model for elucidating key regulatory steps and mechanisms controlling the collagen fiber organization that is critical to determining tissue form and function.

Abbreviations:

3D Three-dimensionally

E Embryonic Day

FFT Fast Fourier Transform

IOP Intraocular Pressure

SHG Second Harmonic Generation

1. Introduction

While the mechanisms regulating the tissue-specific assembly of collagen fibril diameter and spacing are well established [1-5], collagen fibrils are only the basic building blocks for connective tissues, and require bundling to form groups of fibrils forming fibers that are organized into hierarchical structures in a tissue-specific fashion that dictate tissue form and function, such as the coaxially aligned bundles of collagen fibres in tendon [6-8], the interwoven laminated structure in intervertebral disc [9] and the orthogonally arranged and intertwined collagen lamellae of the cornea [10-15]. Less is known with respect to the temporal and spatial mechanisms (cellular, molecular and mechanical) that regulate the assembly of these hierarchal collagen structures and as stated by Trelstad and Birk in 1984, “the weaving of the body fabric from the warp and woof of the matrix has yet to told [16].”

Specifically, the highly ordered collagen architecture of the corneal stroma provides a model system to unravel these mechanisms and key regulatory steps involved in the collagen macrostructure and tissue architecture required for function. The cornea of the vertebrate eye plays a critical role in vision, serving both as a transparent window and a refractive lens that provides over two thirds of the refractive power of the eye in mammals. The principal parts of the cornea are the corneal epithelium, the corneal endothelium and the corneal stroma, which is comprised predominantly of collagen, making up 90% of the corneal thickness. Using non-linear second harmonic generation (SHG) imaging to 3 dimensionally (3D) map the collagen fiber/lamellar architecture, we have previously shown that there are progressive changes within the macrostructure of the cornea from extant species of different vertebrate clades suggesting evolutionary adaptations to accommodate control of corneal shape and refractive power involving increasing lamellar complexity through branching and anastomosing [10-11].

Although the cellular, molecular and mechanical mechanisms controlling these evolutionarily adaptations remain unknown, the patterning of the corneal stroma is likely determined during embryonic development with variations in stromal organization dependent on the vertebrate species. Tissue morphogenesis is a fundamental developmental process closely coupled with a series of matrix-matrix, matrix-cell and cell-

cell interactions [1,17-21]. In like manner, corneal morphogenesis [22-24] is characterized by a series of morphological and biochemical events that take place as the cornea develops, giving the tissue its unique shape, biomechanical properties, structure and composition [25-31].

In particular, chick corneal morphogenesis has been studied extensively and shown to be dependent on the deposition of an acellular primary stroma synthesized by the corneal epithelium [23,32-36] prior to the inward migration of neural crest cells and the deposition of a secondary stroma by the corneal keratocyte [23,31,33-34,37]. Overall, the consensus view is that the acellular primary stroma serves as a scaffold or template for the production of the secondary corneal stroma by the invading neural crest and that the primary stromal architecture mirrors the adult stromal architecture [23,31,38-39].

Recently, developmental studies of the chick cornea using serial block face scanning electron microscopy have identified keratocyte processes, termed keratopodia, that show synchronized alignment with depositing collagen matrix [40]. In a similar manner to mammalian fibroblast fibripositors, identified in developing tendon and cornea that have been hypothesized to play a role in the assembly and alignment of organized extracellular matrix within specific fibroblast compartments [1,41-42], keratopodia have also been proposed to play a role in the collagen fibril organization during tissue morphogenesis. The appearance of keratopodia suggests that developing chick keratocytes may play a more active role in corneal morphogenesis than the secretion of secondary matrix deposited upon a primary matrix scaffold.

Additional evidence suggesting that keratocytes may play a more active role in determining corneal shape has been provided by studies of Coulombre investigating the role of intraocular pressure (IOP) on the development of corneal curvature [43]. During development, corneal shape begins to diverge from scleral shape after embryonic day 8 (E8), or following invasion of the primary stroma by the corneal keratocytes and the deposition of secondary stroma [43]. Interestingly, intubation of the eye at E4 and the loss of IOP leads to the disruption of eye patterning and the failure of the cornea to bulge out from the sclera [43]. This finding lead Coulombre to propose that mechanical factors associated with expansion of the eye by IOP played a dominant role in the formation of

corneal curvature and shape. Whether IOP has any effect on corneal stromal keratocyte and collagen organization has not been studied.

In this study, the morphogenesis of chick cornea was analysed to determine the role of keratocytes and IOP in the assembly of the adult corneal collagen fibril macrostructure and specifically the organization of groups of fibrils to form collagen fibers or lamellae. Our findings indicate that the complex organization of the stroma develops only after neural crest migration and invasion of the primary stroma regardless of the IOP, and that the temporal changes are consistent with the view that keratocytes deposit and organize *de novo* the mature, adult corneal stroma in higher vertebrates, including birds and mammals without mechanical cues generated by increasing IOP. Further study of this model system will allow for a fuller understanding of the molecular mechanisms guiding the assembly of complex hierarchal collagen fibril macrostructures necessary to control tissue form and function.

2. Materials and Methods

2.1. Chicken Embryos

Fertilized White Leghorn chicken eggs (N=72) were obtained from the AA Laboratory Eggs Inc (Westminster, California, USA) and were incubated at 38˚C in a humidified chamber (G.Q.H. Mgf. Co., Savannah, Georgia.). Embryos were collected at successive stages of development, from embryonic day (E) E8 to E19, and fixed in 2% paraformaldehyde in PBS (pH 7.4). All experiments were conducted in agreement with the Association for Research in Vision and Ophthalmology statement for the use of animals for ophthalmic and vision research.

2.2. Eye Intubation – Reduction of Intraocular Pressure (IOP)

On E3, eggs were cracked and the contents poured into sterile weighing boats and then placed in a humidified chamber at 37ºC using methods previously published [44]. The next day (E4), one end of a 0.4 mm glass capillary tube about ~3 mm in length (Capillary Tube Supplies Ltd, Cornwall, UK) was inserted in the wall of one eye of each embryo, after opening the eye with a 0.5 mm surgical knife at the equator (Ambler Surgical, Exton, PA). The tube remained in place until E15, allowing the escape of vitreous humor from

the eye and thus, the lack of IOP. As a control, an incision was made but no tube was introduced in the wall of the eye. On E15, all eyes were harvested, corneas were dissected and fixed in 4% paraformaldehyde in PBS (pH 7.4). Eye intubation experiments were performed three times, one dozen eggs per experiment.

2.3. Tissue Orientation and Imaging Approach

All samples were dissected, orientated and processed the same way in respect to the choroid fissure, a fixed anatomic point in the developing optic cup. Embryonic corneas were examined by both en face and cross-section (transverse) tissue imaging approaches. For en bloc tissue imaging (Figure 1), corneas were mounted on the sample holder, epithelial side down, and through-focus image stacks were taken from the epithelial towards the endothelial surface (A). For cross-sectional imaging (B), excised corneas were embedded in 10% low melting point agarose (NuSieve GTG; Lonza, Rockland, ME, USA), and tissue sections of 200-250 µm thick were cut using a vibratome (Campden Instruments Ltd.).

2.4. SHG Imaging and Confocal Microscopy

Non-linear optical SHG imaging and confocal microscopy were used to investigate the collagen and keratocyte 3D organization in the embryonic chick corneal stroma, respectively. Whole-mount corneas from E8 to E19 were stained en bloc with propidium iodide nucleic acid stain (Excitation/Emission: 493/636 nm; Molecular Probes) and phalloidin (Alexa Fluor 488 phalloidin; Excitation/Emission: 495/519 nm; Molecular Probes) in TD buffer consisting of 0.5% dimethyl sulfoxide, 0.5% Triton X and 2.5% Dextran 40 in PBS, pH 7.4 to identify nuclei and cell cytoskeleton, respectively. Samples were imaged on a Zeiss LSM 510 (LSM 510; Carl Zeiss Inc., Thornwood, NY, USA). To generate SHG signals, the Chameleon laser (Chameleon®, Coherent Incorporated, Santa Clara, California) was tuned to 820 nm and forward and backward scattered signals acquired using the transmitted light detector with a 430 SP filter and a band pass filter, 390/465, respectively. Fluorescence detection of phalloidin and propidium iodide nucleic acid stain was obtained using the 488 nm laser line of the argon ion laser and the BP 500-530 and LP 560 emission filters. 3D image stacks were generated by obtaining through-focus images at 2 µm step intervals, extending from the epithelial towards the

endothelial surface using a X40/1.1 NA water immersion Zeiss Apochromat objective (Carl Zeiss) at a resolution of 512 by 512 pixels per image and with a lateral resolution of 0.44 µm per pixel. For each sample, at least three regions were examined and at least three corneas per embryonic stage were analysed. Experimental settings (i.e pinhole size, exposure time, gain, scan time, dwell time, etc) were kept constant throughout the experiment.

2.5. Fast Fourier Transform (FFT) Analysis and 3D Reconstruction

Collagen and keratocyte angular displacement in the corneal stroma during embryogenesis were assessed by generating 2D fast fourier transforms (FFT) for each plane of the through-focus series dataset using a custom-written software for Image J [45] (http://imagej.nih.gov/ij/) provided in the public domain by the National Institutes of Health, Bethesda, MD, USA). The FFTs display the predominant directions of the collagen and keratocytes in each image plane. The generated 2D FFT images were then assembled together into a new dataset and the angle measurement tool in Image J was utilized to measure the angular offset between adjacent lamellae, as well as the angular displacement of the keratocytes, throughout the entire manually segmented stack of 2D FFT dataset. More precisely, by using the angle measurement tool, the angular offset in the first plane (i.e. x plane) was measured and by keeping one of the two intersecting lines fixed you can then measure how much it has rotated between each plane (i.e. x + n plane). The percentage of stroma that shows keratocyte and/or collagen angular displacement over the total stromal thickness was determined at each embryonic stage. The angular measurements were repeated three times and the average ± standard error (SE) were then calculated from at least four distinct corneas for each developmental day (n= 4-7). The predominant orientations of the 2D FFT image stacks were manually segmented and 3D reconstructed models were created by using Amira software (Visage Imaging, Carlsbad, CA, USA).

Data was further subjected to Fourier component analysis for directionality by the Image J plugin Directionality (http://pacific.mpi-cbg.de/wiki/index.php/Directionality) to assess and quantify the alignment of the collagen and keratocytes at different angles within the image. The intensity of the signal was integrated at different angles (from -90° to 90°) and

expressed as a percentage. 3D directionality plots were then generated using SigmaPlot13 (Systat Software, San Jose, CA) to show the collagen/keratocyte alignment across the corneal stromal depth with development.

2.6. Statistical Analysis

From the through-focus datasets, average collagen angular displacement, keratocyte angular displacement and percentage of the rotated corneal stroma over the total stromal thickness for each developmental day (n= 4-7 per developmental day) were used for statistical analysis using SigmaStat Version 4.0 (Systat Software, San Jose, CA). Shapiro-Wilk normality test and Brown-Forsythe equal variance test were performed followed by a one-way analysis of variance (ANOVA) and Holm-Sidak multiple comparisons test.

2.7. Supplementary Material

Video 1 shows the manually segmented stacks of 2D FFT of collagen corneal stromal organization at E8 and E9. Videos 2 and 3 show the through-focus SHG data, going from the epithelium towards the endothelium, along with the corresponding FFT (inset) and the manually segmented stacks of 2D FFT (green) at E10 and E12, respectively. Video 4 shows the keratocyte organization in the corneal stroma at E8 along with the corresponding FFT (inset) and the manually segmented stack of 2D FFT (red). Video 5 shows the keratocyte through-focus dataset, progressing from the epithelium towards the endothelium, the corresponding FFT dataset (inset) and the manually segmented stack of 2D FFT (red) at E9. Video 6 shows the keratocyte through-focus dataset, progressing from the epithelium towards the endothelium, the corresponding FFT dataset (inset) and the manually segmented stack of 2D FFT (red) at E12.

3. Results

3.1. Collagen Orientation and Angular Displacement

Collagen organization in the embryonic chick cornea was identified by collecting 3D SHG signals from the cornea using high intensity, very short pulsed (femtosecond) laser light. SHG signals in the cornea are generated by fibrillar collagen, which has a non-

centrosymmetric molecular structure capable of frequency doubling photonic radiation in an absorption free, non-linear process that generates a visible light photon when irradiated with infrared laser light [46-47]. Importantly, since collagen molecules are non-centrosymmetrically ordered along the longitudinal axis and centrosymmetrically ordered along their cross-sectional axis, SHG signals only detect fibrils oriented along the optical plane. Furthermore, due to the limits of optical microscopy, structures imaged by SHG are generally larger than 1 μm and therefore represent bundles of collagen fibrils, comprising larger collagen fiber bundles, called lamellae in the cornea [48-50]. These properties of SHG imaging allow for the specific detection of in-plane collagen fibers and the precise measurement of their orientation [51-57]. This is more clearly shown in Figure 1, which depicts SHG imaging of the developing chick cornea at E17. As stated above, the adult corneal stroma is a remarkably ordered structure of orthogonally aligned collagen, which displays a characteristic rotation of the lamellae through the anterior-mid stroma due to the angular displacement between different orthogonal layers. This orthogonal/rotated collagen fibril pattern in the chick corneal stroma is illustrated in en face SHG imaging (A) and the corresponding FFT, showing a shift in the predominant lamellar orientations between 52 μm and 88 μm depths. Rotation of lamellae is also detected in the vibratome sections (B), where an SHG signal is only detected when the collagen lamellae are 'in plane'.

In investigating early embryonic chick corneal collagenous fibrillar extracellular matrix structure during deposition of the primary stroma, no rotation of collagen fibrils was evident at E8 and E9 of corneal development as shown by the en face, single plane SHG images and their corresponding FFT analysis (inset) taken at different depths (Figure 2, Supplementary Video 1). However, the first collagen fibril angular displacement in anterior stroma was detected on E10 (Figure 3, left panel) and averaged 64.5 ± 3.9º within the anterior 36.8 ± 4.7 μm (32.2 ± 3.8 % depth) of the corneal stroma (Supplementary Video 2). The remaining 68.2 % of stroma maintained an orthogonal lamellar orientation, but without any angular displacement/rotation. From E10 to E12 there was a statistically significant increase in both the amount of collagen fibril angular displacement, as well as in the thickness of the rotated stroma up to E12 ($P < 0.001$); so that by E12, the angular displacement of lamellae averaged 155.3 ± 5.6º in the anterior 89.4 ± 7.6 μm of stroma

(55.1 ± 3.5 % depth) (Figure 3, middle panel; Supplementary Video 3). From E12 to E14 there was no significant change in the total angular displacement of lamellae in the anterior stroma (155.3 ± 5.6º versus 155.1 ± 10.0º) or in the percentage of the rotated stroma over the total stromal thickness (55.1 ± 3.5 % versus 51.0 ± 2.15 %). By E19 the developing corneas averaged 193.4 ± 4.1º of lamellar rotation in the 144.3 ± 11.7 µm of anterior stroma (65.1 ± 7.6 %) (data not shown).

To further define the rotation of collagen lamellae with development, the level of collagen fiber alignment was quantitatively assessed using the Image J Directionality plugin. Figure 4 shows the integrated collagen SHG signal as a function of corneal depth, plotted as a percentage against different angles (from -90° to +90°). Prior to E10, there are three well-defined peaks at -90°, at 0° and at +90°, consistent with an orthogonal organization of collagen lamellae. A single peak at 0° extends throughout the cornea, showing the absolute orientation of the orthogonal collagen layers with respect to the choroid fissure; with one axis parallel to, and the other perpendicular to the choroid fissure. There is no shift in the peaks of the preferred collagen alignment, indicating no rotation of collagen lamellae. By E10 there is a clear rotational shift in the alignment of collagen within the anterior stroma starting at a depth of around 40 µm. From E10 onwards, more peaks emerge at different angles that have shifted from 0°, representative of an increase in collagen angular displacement in the anterior-mid stroma with development. Note that the posterior stroma always displays three peaks (-90°, 0°, +90°), associated with an orthogonal/non-rotational lamellar organization.

The data regarding rotation of lamellae starting at E10 was also extended by SHG imaging of sections allowing deeper tissue evaluation as shown in Figure 5. In cross section, an SHG signal from collagen will only be generated if the collagen lamellae are oriented in the same optical plane as the SHG imaging. Vibratome sections of E8 and E9 corneas showed a homogeneous SHG signal throughout the corneal thickness indicating that no collagen lamellae were oriented along the image plane. However, at E10, an SHG signal was detected in the anterior stroma, averaging 14.5 ± 0.6 µm below the corneal epithelium. This finding indicates that the collagen lamellae in the anterior stroma must have undergone a rotation of more than 45º with respect to tissue above. This is

consistent with the measured rotation from en face data of 63.2º. By E12, two SHG bands were detected within the corneal stroma at 22.3 ± 3.2 μm and 69.4 ± 4.9 μm depth. Given the orthogonal arrangement of collagen lamellae, the appearance of two bands indicates that the collagen lamellae deposited between them must have rotated at least 90º. This again is consistent with the rotational analysis of the en face data, which shows a total rotation of 155.3º, which is greater than the minimum rotation 135º (90º + 45º) needed to see the two bands. No change in the number of bands was detected at E14, which again is consistent with the en face data, showing no additional rotation. However, it should be noted that the bands appear more distinct at E14 and the cornea is thinner. The decreased corneal thickness is consistent with the beginning of corneal compaction and the stronger signal may be associated with the closer alignment of collagen lamellae due to this compaction. Rotation of collagen lamellae also led to the development of a complex structural organization by E18 consisting of highly interconnected collagen lamellae with extensive branching and anastomosing (Figure 6) that is characteristic of adult 'chicken-wire' corneal structure [11].

3.2. Mechanical forces, generated by increasing intraocular pressure (IOP) do not influence collagen fibril macrostructure organization

Previous studies have shown that eye development is dependent, in part, on IOP and that intubation of the eye at E4 inhibits eye growth and the normal development of the cornea [43, 58-59, 58-61]. To determine whether the collagen fibril macrostructure and tissue architecture in the corneal stroma are similarly affected by IOP, developing chick eyes were intubated at E4 and allowed to develop to E15. As shown in Figure 7, the intubated eyes (Figure 7A and C) where the tube remained in place to E15 (arrow), the loss of IOP inhibited the growth of the eye and cornea compared to the opposite, non-intubated, control eye (Figure 7B and D). As previously reported by others, the transparency of the corneas was not affected by eye intubation but did result in the development of a small lens and severely folded retina [43, 58-59]. The collagen fibril macrostructure in the absence of IOP was similar between the control eye the intubated eye, both showing 120º of rotation at E15 (Figure 7E and F). While this rotation is less than that measured for corneas develop *in ovo*, the similar rotation between control and

intubated eyes indicate that the decreased rotation was due to the environmental difference between *ex ovo* and *in ovo* development rather than loss of IOP.

3.3. Keratocyte Orientation and Angular displacement

Taking into consideration that previous studies suggested that the primary stroma provides essential cues for cell migration and alignment, keratocyte morphology and orientation in the developing stroma was investigated. Initial cell migration begins around day E5½, when neural crest/presumptive keratocytes invade the middle and posterior layers of the primary corneal stroma. Keratocytes continue to invade the acellular primary stroma beneath the basal layer of the corneal epithelium (Figure 8A, arrowheads) and show full invasion by E10 (Figure 8A).

At E8, most cells appeared to be randomly oriented within the anterior-mid stroma, while cells in the posterior stroma showed a preferential parallel orientation aligned with the choroid fissure (Figure 8B, left panel; Supplementary Video 4). One day later (E9), keratocytes developed an orthogonal orientation in the anterior 45.3 ± 3.5 μm of the stroma (38.8 ± 4.5 % depth) and displayed a clockwise rotation of 59.3 ± 7.1º (Figure 8B, right panel; Supplementary Video 5). From E10 onwards, keratocytes were orthogonally orientated and displayed a significantly greater rotation (109.8 ± 4.5º ; $P < 0.001$) within the anterior corneal stroma (45.9 ± 5.2 % depth) (Figure 9; Supplementary Video 6). Table 1 presents the degree of keratocyte angular displacement, along with the percentage of the rotated stroma over total stromal thickness during corneal development. Similar to collagen angular displacement, there was no additional rotation of cells detected between E12-E14 during early corneal compaction. Thereafter, the angular displacement of the keratocytes increases so that by E19 the keratocytes display an angular displacement of 201 ± 5.2º in the 168.5 ± 6.6 μm (75.4 ± 4.0 % depth) of the embryonic chick corneal stroma. Thereafter, the angular displacement of the keratocytes increases so that by E19 the keratocytes display an angular displacement of 201 ± 5.2º in the 168.5 ± 6.6 μm (75.4 ± 4.0 % depth) of the embryonic chick corneal stroma.

To obtain an additional quantitative measure of the level of organization of keratocytes throughout the corneal stroma with development, through-focus datasets were subjected to Directionality analysis using Image J Directionality plugin. Directionality analysis,

representing the percentage of signal/keratocytes aligned along a particular direction (Figure 10), showed that at E8 the keratocytes are aligned in respect to the choroid fissure (peak at 0º), as well as at different angles (peaks ranging from -90º to +90º), indicating that while some keratocytes are orthogonally arranged, there is predominantly a random organization. At E9, more peaks emerge at -90º, 0º and +90º suggesting that keratocytes take up a more orthogonal organization with respect to the choroid fissure. Additionally, in the anterior stroma the peaks show a shift from 0º, denoting rotation of the keratocytes. This shift does not appear in the posterior stroma, indicating that the keratocytes only rotate in the anterior stroma. From E10 onwards, there is a gradual increase in the shift of the peaks of the preferred alignment of keratocytes at various angles suggestive of an enhanced keratocyte angular displacement in the anterior stroma. Note that a percentage of keratocytes in the posterior stroma always aligns at -90º, 0º and +90º, indicating no rotation.

3.4. Keratocyte - Collagen organization in the embryonic chick corneal stroma

To better visualize changes in the keratocyte and collagen angular displacement during corneal development, the FFTs for each plane from the SHG and keratocyte en face datasets at different developmental days were assembled into image stacks, segmented and subsequently rendered in 3D. Figure 11A shows representative manually segmented stacks of 2D FFTs of keratocytes (red) and SHG (green) stacks from the same corneas to demonstrate the predominant directionality throughout the corneal thickness. Each spoke highlights the principal orientation for each lamellae or cell within that plane. On E8, the keratocyte orientation appears predominantly random through the full stromal thickness, reflected by the absence of any distinct spokes. On the same day (E8), the collagen orientation is orthogonal through the entire stroma and does not display any angular displacement between adjacent lamellae. On E9, keratocytes show a rotational pattern in the anterior stroma, while the collagen organization within the same cornea shows no rotation between adjacent lamellae. On E10 the first rotation appeared in the manually segmented stacks of 2D FFTs of SHG in the anterior stroma, which as the cornea develops extends throughout the mid stroma but not the posterior stroma.

To better compare the rotational organization of keratocytes and collagen in the embryonic chick corneal stroma, the average angular displacement (n=4-7) of keratocytes (red) and collagen (green) as a function of corneal development was plotted (Figure 11B). In addition, the percentage of rotated stroma over total stromal thickness as a function of embryonic development in the same eyes was also plotted (Figure 11C). Table 1 summarizes the changes in angular displacement of keratocytes and collagen lamellae, as well as the percentage of the rotated stroma over total stromal thickness during corneal development. The angular displacement of keratocytes on E9 was significantly different from that of collagen at E9 and remained significantly different from E10 to E12 ($P < 0.001$). The angular displacement of keratocytes on E9 was significantly different from that of collagen at E9 and remained significantly different from E10 to E12 ($P < 0.001$). From E14 onwards there was no significant difference between the angular displacement of keratocytes and collagen. Hence, although keratocyte rotation precedes collagen rotation (begins on E9 opposed to E10), the keratocyte and collagen angular displacement with stromal depth synchronizes in the developing matrix by E14.

Discussion

Collagen is the major component of connective tissues and extracellular matrix. While the cellular and molecular mechanisms of collagen fibrillogenesis are well known [1-5], connective tissue structure and function are intimately associated with the specific spatial organization of collagen fibrils as organized into bundles, fibers and larger structures, such as lamellae [41]. Although special attention has been paid to the intrinsic physical self-assembly property of collagen in vitro [62-66], the mechanisms and regulatory steps that drive fibril bundling, interweaving and intertwining to form tissue-specific hierarchal structures that define tissue form and function are unknown.

In this study we have used the chick embryonic corneal stroma as a model system to begin to identify the cellular and mechanical mechanisms that control hierarchical assembly of collagen in the adult cornea. Our findings indicate that the adult corneal structural organization that is comprised of rotating collagen fibers with branching and anastomosing begins to develop at E10, after full invasion of the corneal stroma by keratocytes. The initiation of adult corneal morphogenesis at E10 is also supported by the

cross-section SHG imaging, which shows a band at E10 and two bands from E12 onwards. These findings together indicate that the more complex, adult collagen fibril macrostructure is sequentially deposited by the corneal keratocytes. Our findings run counter to the prevailing view that the adult chick corneal structure is controlled and guided by the corneal epithelium [31], although this is likely the case for lower vertebrate corneas that show a simple 'plywood' collagen organization. However, the more complex structural organization necessary to control corneal shape and refractive power that is observed in higher vertebrates, including birds and mammals, would seem to require the presence of corneal keratocytes that potentially orchestrate the complex branching and anastomosis patterns seen in these species.

In evaluating potential mechanisms, previous studies by Coulombre and Coulombre in 1958 identified IOP as playing an important role in controlling eye growth and corneal shape [58-59], and that intubation of the eye to block the development of IOP leads to the formation of a small, spherical eye with the cornea and sclera having the same radius of curvature [43]. In these studies, it was noted that corneal curvature begins to diverge from that of the scleral curvature at E8, a similar developmental time point associated with the change from a random to orthogonal orientation of keratocytes and the later deposition of rotational collagen [43]. While it is not clear how IOP might control corneal shape, our finding that loss of IOP had no effect on the keratocyte and collagen orthogonality indicates that IOP does not influence this process. Since IOP only influences eye patterning and not cell differentiation as noted by Coulombre [43], the factors controlling stromal organization are likely due to keratocyte differentiation. This notion is supported by seminal studies by Ruberti and colleagues who demonstrated that human keratocytes can produce an orthogonal, three-dimensional matrix that resembles the corneal stromal architecture [67-69]. This further advocates that the directionality of the mechanical stimuli, which are likely very weak in an expanding cornea, cannot override the patterning behaviour of the corneal stromal cells.

Interestingly, our data evaluating keratocyte orientation during corneal development demonstrates that while keratocytes show a predominantly random organization at E8,

by E9 they develop an orthogonal arrangement and clockwise rotation in the anterior stroma. As development progresses, there is a gradual increase in the angular displacement of keratocytes within the corneal stroma, which synchronizes with the collagen angular displacement, evocative of a keratocyte-collagen interrelationship [70]. A possible explanation for this phase lag between the rotation of keratocytes and the stromal collagen is that in the developing tissue, the extracellular matrix is comprised of several other molecules, which regulate collagen organization and collagen fibrillogenesis that are not detected by SHG [71-72]. Similarly, non-fibrillar collagen cannot be detected by SHG and since tissue morphogenesis is a dynamic process, where matrix secretion and organization take place, it is possible that the phase lag is attributed to biosynthesis, enzymatic processing of the procollagen and organization [64]. In support of this statement, previous studies demonstrated that corneal and scleral collagen type I fibrillogenesis, in the presence of proteoglycans, is retarded in rate in vitro [73]. An alternative possibility is that following realignment of the keratocytes the matrix undergoes remodeling and realignment, however, how this would be controlled is not clear.

The fact that keratocyte rotation precedes that of collagen further supports a role for the keratocytes in the organization of the mature corneal collagen stromal architecture. While the posterior secondary stroma follows the orthogonal collagen organization of the primary stroma, the more complex anterior secondary stroma having increased collagen branching and anastomosis appears to be deposited *de novo* or as a replacement of the primary stroma and not simply the addition to an already complex structure. This concept finds some support in previous studies by Birk and Trelstad who proposed that collagen fibril, bundle and lamellar assembly is driven by keratocytes via specific extracellular compartments, which are aligned along the fibroblasts [1,41]. The recent identification of actin-associated tubular keratocyte protrusions, termed keratopodia, which exhibit long-range associations with collagen in the corneal stroma and reflect the alignment of collagen and emergent lamellae [40] further suggest that keratocytes play a more active role in the organization of the corneal collagen stromal architecture.

The cellular influence on the orientation of the collagen that it is deposited has been frequently noted [23,74-79]. Studies by Wang and colleagues indicate that the matrix

organization may be dependent on the cell orientation supporting the effect of cell orientation on the alignment of collagen seen in this study [80]. During corneal development, keratocyte morphology changes depending on the embryonic day, as well as the position in the stroma [23,81]. For instance, at E10, keratocytes near the epithelium are more rounded, whereas posteriorly they are more elongated. Evidently, the mechanical stimuli exerted by the IOP in the plane of the cornea, do not override cell patterning. This notion is supported by previous studies by Doane and Birk, 1991 who demonstrated that fibroblasts retain their cellular and tissue phenotype in the absence of load in vitro, with corneal fibroblasts producing orthogonal patterns, tendon fibroblasts orientating parallel to each other and dermal fibroblasts showing no apparent orientation [82]. This idea is additionally supported by in vitro studies of primary human corneal fibroblasts cultured in an unloaded model system and shown to synthesize a highly organized collagenous matrix [67]. This raises the question as to what drives these keratocyte morphological changes during corneal embryogenesis. The importance of biophysical and topographical cues in modulating cellular mechanics, secretion and organization of extracellular matrix has been frequently noted [67-69, 83-88], however, it remains to be determined if the keratocyte morphological changes in the developing cornea are attributed to mechanical, biophysical and/or topographical cues. Intriguingly, it has recently shown that corneal fibroblasts are highly sensitive to uniaxial global and applied mechanical stimuli [69].

One possible alternative mechanism through which keratocytes may drive the development of a complex interconnected network of collagen involves the cornea as an autonomous, self-propagating chemical system where protein synthesis and matrix organization remains nearly constant. This property is reflected by several physicochemical variations that correlate with alterations in corneal structure-function relationships; such as the enzymatic activity of hyaluronidase which takes place between E9-E14, associated with dehydration and compaction of the corneal stroma [31]. Also changes in the chemical composition [89-90] and proteoglycan/glycosaminoglycan content of the cornea with development may also play a role [91-95]. It is, therefore, likely that keratocytes may respond to chemical and/or mechanical cues within the embryonic

tissue environment that lead to the initiation of branching and anastomosing and ultimately the morphogenesis of the adult corneal stroma.

The questions of why do keratocytes display a gradual clockwise rotation and what are the factors that depict their organization during corneal development remain to be elucidated. Future studies mapping cell-cell interactions, cell-matrix interactions and how various stimuli, both internal and external, are integrated within the embryonic corneal tissue environment, may perhaps address the exact mechanisms by which cell and collagen organization is established.

4. Conclusions

In summary, the current study investigated the morphologic and structural changes coupled with the emergence of collagen fibril bundle formation and macrostructure in the corneal stroma during development using 3D collagen imaging via SHG and confocal microscopy. The findings presented here propose a new role for keratocytes in the more complex collagen organization of the adult corneal matrix. This new role provides a convergence in the morphogenetic and developmental pathways between higher non-mammalian vertebrates and mammals that lack a primary stroma and are dependent on keratocytes for the structural organization of the stroma. This convergence also provides a stronger foundation of the development of stromal complexity in controlling corneal shape and refractive power. Although a number of potential mechanisms have been put forward to explain matrix organization during corneal development, more work is required to fully elucidate the exact mechanisms as to how collagen tissue-specific fibril macrostructure organization is directed, sustained and regulated; important consideration for future tissue engineering and regenerative medicine applications. Clearly understanding the cellular and molecular mechanisms that regulate keratocyte directed, collagen macrostructure may additionally help in elucidating the underlying mechanisms associated with the development of refractive errors such as myopia, hyperopia and astigmatism. In this regard, the avian cornea with its high degree of structural complexity may be a valuable experimental model upon which these mechanisms can be elucidated.

Acknowledgements

Supported by the Biotechnology and Biological Sciences Research Council Grant - BBSRC Grant, BBSRC BB/M025349/1 (AJQ), the NIH NEI EY024600 (JVJ), Research to Prevent Blindness, Inc. The Skirball Program in Molecular Ophthalmology. The authors would like to thank Yilu Xie and Kelly Huynh for their support with this project.

References

1. Birk DE and Trelstad RL. 1986. Extracellular Compartments in Tendon Morphogenesis: Collagen Fibril, Bundle, and Macroaggregate Formation. J Cell Biol. 103; 231-340
2. Chakravarti S, Petroll WM, Hassell JR, Jester JV, Lass JH, Paul J, Birk DE. 2015. Corneal opacity in lumican-null mice: Defects in collagen fibril structure and packing in the posterior stroma. Invest Ophthalmol Vis Sci. 41: 3365-3373
3. Holmes DF, Gilpin CJ, Baldock C, Ziese U, Koster AJ, Kadler KE. 2001. Corneal collagen fibril structure in three dimensions: Structural insights into fibril assembly, mechanical properties, and tissue organization. Proc Nat Acad Sci. 98 (13) 7307-7312
4. Miyahara M, Hayashi K, Berger J, Tanzawa K, Njieha FK, Trelstad RL, Prockop DJ. 1984. Formation of collagen fibrils by enzymic cleavage of precursors of type I collagen in vitro. J Biol Chem. 259; 9891-9898
5. Orgel JPRO, Antipova O, Sagi I, Bitler A, Qiu D, Wang R, Xu Y, San Antonio JD. 2011. Collagen fibril surface displays a constellation of sites capable of promoting fibril assembly, stability and hemostasis. Connect Tissue Res. 52: 18-24
6. Birk DE, Zycband EI, Woodruff S, Winkelmann DA, Trelstad RL. 1997. Collagen fibrillogenesis in situ: fibril segments become long fibrils as the developing tendon matures. Dev Dyn. 208: 291-298
7. Provenzano PP and Vanderby RJ. 2006. Collagen fibril morphology and organization: implications for force transmission in ligament and tendon. Matrix Biol. 25: 71-84
8. Glimcher MJ and Katz EP. 1965. The organization of collagen in bone: the role of noncovalent bonds in the relative insolubility of bone collagen 1. J Ultrastruct Res. 12: 705-729
9. Hayes AJ, Isaac MC, Hughes C, Caterson B, Ralphs JR. 2011. Collagen fibrillogeneis in the development of the annulus fibrosus of the intervertebral disc. European Cells and Materials. 22: 226-241

10. Koudouna, E., Winkler, M., Mikula, E., Juhasz, T., Brown, DJ., Jester, JV., 2018. Evolution of the vertebrate corneal stroma. *Prog Retin Eye Res*. https://doi.org/10.1016/j.preteyeres.2018.01.002
11. Winkler M, Shoa G, Tran ST, Xie Y, Thomasy S, Raghunathan VK, Murphy C, Brown DJ, Jester JV. 2015. A comparative study of vertebrate corneal structure: The evolution of a refractive lens. Investigative Ophthalmology & Visual Science. 56: 2764-2772
12. Jester JV, Winkler M, Jester BE, Nien C, Chai D, Brown DJ. 2010. Evaluating corneal collagen organization using high resolution non linear optical (NLO) macroscopy. Eye Contact Lens. 36: 260-264
13. Morishige N, Petroll WM, Nishida T, Kenney MC, Jester JV. 2006. Noninvasive corneal stromal collagen imaging using two-photon-generated second-harmonic signals. Journal of Cataract & Refractive Surgery. 32: 1784-1791
14. Winkler M, Chai D, Krilling S, Nien CJ, Brown DJ, Jester B, Juhasz T, Jester JV. 2011. Nonlinear optical macroscopic assessment of 3-D corneal collagen organization and axial biomechanics. Investigative Ophthalmology & Visual Science. 52: 8818-8827
15. Winkler M, Shoa G, Xie Y, Petsche SJ, Pinsky PM, Juhasz T, Brown DJ, Jester JV. 2013. Three-dimensional distribution of transverse collagen fibers in the anterior human corneal stroma. Investigative Ophthalmology & Visual Science. 54: 7293-7301
16. Trelstad RL, Birk DE. Collagen fibril assembly at the surface of polarized cells. In: Trelstad RL, editor. The role of extracellular matrix in development. Alan R. Liss, Inc.; New York: 1984. pp. 513–543.
17. Birk, D.E., Zycband, E.I., Winkelmann, D.A., Trelstad, R.L., 1990. Collagen fibrillogenesis *in situ*. Discontinuous segmental assembly in extracellular compartments. Ann NY Acad Sci. 580: 176-194
18. Birk, D.E., Zycband E., 1993. Assembly of the collagenous extracellular matrix during tendon development in the chicken limb. Prog Clin Biol Res. 383B: 523-532
19. Birk, D.E., Zycband E., 1994. Assembly of the tendon extracellular matrix during development. J Anat. 184: 457-463
20. Rozario T, DeSimone DW. 2009. The extracellular matrix in development and morphogenesis: A dynamic view. Developmental Biology 341:126-140
21. Zhang, G., Young, B.B., Ezura, Y., Favata, M., Soslowsky, L.J., Chakravarti, S., Birk, D.E., 2005. Development of tendon structure and function: Regulation of collagen fibrillogenesis. J Musculoskelet Neuronal Interact. 5: 5-21
22. Chen, S., Mienaltowski, M.J., Birk, D.E., 2015. Regulation of corneal stroma extracellular matrix assembly. Exp Eye Res. 133: 69-80
23. Hay ED, Revel J-P. 1969. Fine structure of the developing avian cornea. In: Wolsky A, Chen PS, editors. Monographs in developmental biology. Vol. 1. Basel: S. Karger. p 1-144

24. Quantock AJ, Young RD. 2008. Development of the corneal stroma, and the collagen-proteogylcan associations that help define its structure and function. Developmental Dynamics. 237: 2607-2621
25. Anseth A. 1961. Glycosaminoglycans in the developing corneal stroma. Experimental Eye Research. 1: 116-121.
26. Conrad GW. 1970. Collagen and mucopolysaccharide biosynthesis in the developing chick cornea. Developmental Biology. 21: 292-317
27. Coulombre AJ, Coulombre JL. 1958. Corneal Development. I. Corneal transparency. Journal of Cellular Physiology. 51: 1-11
28. Coulombre AJ, Coulombre JL. 1961. The development of the structural and optical properties of the cornea. In: Smelser GK, editor. The structure of the eye. London and New York: Academic Press. p 405-420
29. Linsenmayer TF, Fitch JM, Gordon MK, Cai CX, Igoe F, Marchant JK, Birk DE. 1998. Development and roles of collagenous matrices in the embryonic avian cornea. Progress in retinal and eye research. 17: 231–265.
30. Toole BP, Trelstad RL. 1971. Hyaluronate production and removal during corneal development in chick. Developmental Biology. 26: 28-35
31. Trelstad RL, Coulombre AJ. 1971. Morphogenesis of the collagenous stroma in the chick cornea. Journal of Cell Biology. 50: 840-858
32. Conrad GW, Paulsen AQ, Luer CA. 1994. Embryonic development of the cornea in the eye of the clearnose skate, *Raja eglanteria*: I. Stromal development in the absence of an endothelium. Journal of Experimental Zoology. 269: 263-276
33. Hay ED and Dodson JW. 1973. Secretion of collagen by corneal epithelium. I. Morphology of the collagenous products produced by isolated epithelia grown on frozen-killed lens. The Journal of Cell Biology. 57: 190-213
34. Hayashi M, Ninomiya Y, Hayahsi K, Linsenmayer TF, Olsen BR, Trelstad RL. 1988. Secretion of collagen types I and II by epithelial and endothelial cells in the developing chick cornea demonstrated by in situ hybridization and immunohistochemistry. Development. 103: 27-36
35. Svoboda, K.K., 1991.Intracellular localization of types I and II collagen mRNA and endoplasmic reticulum in embryonic corneal epithelia. J Cell Sci. 100: 23-33
36. Svoboda, K.K., Nishimura, I., Sugrue, S.P., Ninomiya, Y., Olsen, B.R., 1988. Embryonic chicken cornea and cartilage synthesise type IX collagen molecules with different amino-terminal domains. Proc Natl Acad Sci USA. 85(20):7496-7500.
37. Meyer DB and O'Rahilly R. 1959. The development of the cornea in the chick. Development. 7: 303-315
38. Coulombre AJ. 1965. Problems in corneal morphogenesis. Advances in Morphogenesis. 4: 81-109

39. Trelstad RL. 1982. The bilaterally asymmetrical architecture of the submammalian corneal stroma resembles a cholesteric liquid crystal. Developmental Biology. 92: 133-134
40. Young RD, Knupp C, Pinali C, Png KMY, Ralphs JR, Bushby AJ, Starborg T, Kadler KE, Quantock AJ. 2014. Three-dimensional aspects of matrix assembly by cells in the developing cornea. Proceedings of the National Academy of Sciences of the United States of America. 111: 687-692
41. Birk DE, Trelstad RL. 1984. Extracellular compartments in matrix morphogenesis: collagen fibril, bundle, and lamellar formation by corneal fibroblasts. The Journal of Cell Biology. 99: 2024-2033
42. Canty EG, Yinhui L, Meadows RS, Shaw MK, Holmes DF, Kadler KE. 2004. Coalignment of plasma membrane channels and protrusions (fibripositors) specifies the parallelism of tendon. The Journal of Cell Biology. 165: 553-563
43. Coulombre, A.J., and Coulombre, J.L., 1958. The role of intraocular pressure in the development of the chick eye. IV. Corneal Curvature. A.M.A. Archives of Opthalmology. 59: 502-506
44. Cloney, K., and Franz-Odendaal, T.A., 2015. Optimized ex-ovo culturing of chick embryos to advanced stages of development. J Vis Exp. 95: e52129, doi:10.3791/52129
45. Schneider CA, Rashband WS. Eliceiri KW. 2012. NIH Image to ImageJ: 25 years of image analysis. Nature Methods. 9: 671-675
46. Franken P, Hill A, Peters C, Weinreich G. 1961. Generation of optical harmonics. Phys Rev Lett. 7: 118–119.
47. Goppert-Mayer M. 1931. Uber Elementarakte mit zweit quantensprungen. Ann Phys. 9: 273–294.
48. Komai Y., Ushiki T. 1991. The three-dimensional organisation of collagen fibrils in the human cornea and sclera. Invest. Ophthalmol. Vis. Sci. 32: 2244–2258.
49. Meek, KM., and Knupp, C., 2015. Corneal structure and transparency. Prog Retin Eye Res. 49: 1-16
50. Polack, F., 1961. Morphology of the cornea. 1. Study with silver stains. Am. J. Ophthalmol. 51: 1051–1056
51. Aptel F, Olivier N, Deniset-Besseau A, Legeais JM, Plamann K, Schanne-Klein MC, Beaurepaire E. 2010. Multimodal nonlinear imaging of the human cornea. Invest Ophthalmol Vis Sci; 51: 2459-2465
52. Campagnola PJ, Millard AC, Terasaki M, Hoppe PE, Malone CJ, Mohler WA. 2002. Three-dimensional high-resolution second-harmonic generation imaging of endogenous structural proteins in biological tissues. Biophys J. 82: 493-508
53. Campagnola P. 2011. Second harmonic generation imaging microscopy: Applications to disease diagnostics. Anal Chem. 83: 3224-3231

54. Campagnola PJ and Dong C-Y. 2009. Second harmonic generation microscopy: principles and applications to disease diagnosis. Laser Photon Rev. 5: 13-26
55. Chen X, Nadiarynkh O, Plotnikov S, Campagnola PJ. 2012. Second harmonic generation microscopy for quantitative analysis of collagen fibrillar structure. Nat Protoc. 7: 654-669
56. Han M., Giese G., Bille J.F. 2005. Second harmonic generation imaging of collagen fibrils in cornea and sclera. Opt. Express 13: 5791–5797
57. Williams RM, Zipfel WR, Webb WW. 2005. Interpreting second-harmonic generation images of collagen I fibrils. Biophys J. 88: 1377-1386
58. Coulombre, A.J., 1956. The role of intraocular pressure in the development of the chick eye. I. Control of eye size. J Exp Zool. 133: 211-225
59. Coulombre, A.J., 1957. The role of intraocular pressure in the development of the chick eye. II. Control of corneal size. A.M.A. Archives of Opthalmology. 57: 250-253
60. Coulombre, A.J., Steinberg, S.N., Coulombre, J.L., 1963. The role of intraocular pressure in the development of the chick eye. V. Pigmented epithelium. Invest Opthalmol Vis Sci. 2: 83-89
61. Neath, P., Roche, S.M., Bee, J.A., 1991. Intraocular pressure-dependent and –independent phases of growth of the embryonic chick eye and cornea. Invest Opthalmol Vis Sci. 32: 2483-2491
62. Giraud-Guille MM, Besseau L, Martin R. 2003. Liquid crystalline assemblies of collagen in bone and in vitro systems. J Biomech; 36: 1571-1579
63. Giraud-Guille MM, Mosser G, Belamie E. 2008. Liquid crystallinity in collagen systems in vitro and in vivo. Curr Opin Colloid Interface Sci; 13: 303-313
64. Trelstad RL, Birk DE, Silver FH. 1982. Collagen fibrillogenesis in tissues, in solution and from modeling: A synthesis. J Invest Dermatol; 79: 109-112
65. Giraud-Guille MM, Mosser G, Helary C, Eglin, D. 2005. Bone Matrix like Assemblies of Collagen: From Liquid Crystals to Gels and Biomimetic Materials. Micron; 36, 602−608
66. Gobeaux F, Belamie E, Mosser G, Davidson P, Panine P, Giraud-Guille MM. 2007. Cooperative ordering of collagen triple helices in the dense state. Langmuir; 23: 6411-6417
67. Guo X, Hutcheon AEK, Melotti SA, Zieske JD, Trinkaus-Randall V, Ruberti JW. 2007. Morphological Characterization of Organized Extracellular Matrix Deposition by Ascorbic Acid-Stimulated Human Corneal Fibroblasts. Investigative Ophthalmology and Visual Science. 48: 4050-4060
68. Saeidi N, Guo X, Hutcheon AE, Sander EA, Bale SS, Melotti SA, Zieske JD, Trinkaus-Randall V, Ruberti JW. 2012. Disorganized collagen scaffold interferes with fibroblast mediated deposition of organized extracellular matrix in vitro. Biotechnology and Bioengineering. 109: 2683–2698

69. Zareian R, Susilo ME, Paten JA, McLean JP, Hollman J, Karamichos D, Messer CS, Tambe DT, Saeidi N, Zieske JD, Ruberti JW. 2016. Human corneal fibroblast pattern evolution and matrix synthesis on mechanically biased substrates. Tissue Engineering. 22: 1204-1217
70. Bard JBL, Higginson K. 1977. Fibroblast-collagen interactions in the formation of the secondary stroma of the chick cornea. Journal of Cell Biology; 74: 816-827
71. Kadler KE, Hill A, Canty-Laird EG. 2008. Collagen fibrillogenesis: fibronectin, integrins, and minor collagens as organizers and nucleators. Current Opinion in Cell Biology. 20: 495-501
72. Scott JE, Orford CR. 1981. Dermatan sulphate-rich proteoglycan associates with rat tail-tendon collagen at the d band in the gap region. Biochemistry Journal. 197: 213-216
73. Birk DE, Lande MA. 1981. Corneal and scleral collagen fiber formation in vitro. Biochimica et Biophysica Acta. 670: 362-369
74. Porter KR, Pappas GD. 1959. Collagen formation by fibroblasts of the chick embryo dermis. The Journal of Biophysical and Biochemical Cytology. 5: 153-166
75. Trelstad RL. 1970. The Golgi apparatus in chick corneal epithelium: Changes in intracellular position during development. Journal of Cell Biology. 45: 34-42
76. Trelstad RL. 1971. Vacuoles in the embryonic chick corneal epithelium, an epithelium which produces collagen. Journal of Cell Biology. 48: 689-694
77. Bell E, Ivarsson B, Merrill C. 1979. Production of a tissue-like structure by contraction of collagen lattices by human fibroblasts of different proliferative potential in vitro. Proceedings of the National Academy of Science USA. 76: 1274–1278
78. Huang D, Chang TR, Aggarwal A, Lee RC, Ehrlich HP. 1993. Mechanisms and dynamics of mechanical strengthening in ligament-equivalent fibroblast-populated collagen matrices. Annals of Biomedical Engineering. 21: 289–305
79. Eastwood M, Mudera VC, McGrouther DA, Brown RA. 1998. Effect of precise mechanical loading on fibroblast populated collagen lattices: morphological changes. Cell Motility and Cytoskeleton. 40: 13–21
80. Wang JH, Jia F, Gilbert TW, Woo SL. 2003. Cell orientation determines the alignment of cell-produced collagenous matrix. Journal of Biomechanics. 36: 97-102
81. Karamichos D, Funderburgh ML, Hutcheon AEK, Zieske JD, Du Y, Wu J, Funderburgh. 2014. A role for topographic cues in the organization of collagenous matrix by corneal fibroblasts and stem cells. PLoS ONE 9(1): e86260. doi:10.1371/journal.pone.0086260
82. Doane KJ, Birk DE. 1991. Fibroblasts retain their tissue phenotype when grown in three-dimensional collagen gels. Exp Cell Res; 195: 432-442
83. Myrna KE, Mendonsa R, Russell P, Pot SA, Liliensiek SJ, Jester JV, Nealey PF, Brown D, Murphy CJ. 2012. Substratum topography modulates corneal fibroblast to myofibroblast transformation. Invest Ophthalmol Vis Sci; 53: 811-816

84. Petroll WM, Kivanany PB, Hagenasr D, Graham EK. 2015. Corneal fibroblast migration patterns during intrastromal wound healing correlate with ECM structure and alignment. Invest Ophthalmol Vis Sci; 56: 7352-7361
85. Ingber DE. 1993. The riddle of morphogenesis: A question of solution chemistry or molecular cell engineering? Cell. 75: 1249-1252
86. Pizzo AM, Kokini K, Vaughn LC, Waisner BZ, Voytik-Harbin SL. 2005. Extracellular matrix (ECM) microstructural composition regulates local cell-ECM biomechanics and fundamental fibroblast behaviour: a multidimensional perspective. Journal of Applied Physiology. 98: 1909-1921
87. Paluch E, Heisenberg CP. 2009. Biology and physics of cell shape in development. Current Biology. 19: R790-R799
88. Raghunathan, V.K., Thomasy, S.M., Strøm, P., Yañez-Soto, B., Garland, J., Sermeno, J., Reilly, C.M., Murphy, C.J. 2017. Tissue and cellular biomechanics during corneal wound injury and repair. Acta Biomater. 58: 291-301
89. Koudouna E, Veronesi G, Patel II, Cotte M, Knupp C, Martin FL, Quantock AJ. 2012. Chemical composition and sulphur speciation in bulk tissue by x-ray spectroscopy and x-ray microscopy: Corneal development during embryogenesis. Biophysical Journal. 103: 357-364
90. Veronesi G, Koudouna E, Cotte M, Martin FL, Quantock AJ. 2013. X-ray absorption near-edge structure (XANES) spectroscopy identifies differential sulphur speciation in corneal tissue. Analytical and Bioanalytical Chemistry. 405: 6613-6620
91. Zhang, Y., Conrad, A.H., Conrad, G.W., 2005. Detection and quantification of sulphated disaccharides from keratin sulfate and chondroitin/dermatan sulfate during chick corneal development by ESI-MS/MS. Invest Ophthalmol Vis Sci. 46: 1604-1614
92. Liles M, Palka BP, Harris A, Kerr B, Hughes C, Young RD, Meek KM, Caterson B, Quantock AJ. 2010. Differential relative sulfation of Keratan sulfate glycosaminoglycan in the chick cornea during embryonic development. Investigative Ophthalmology & Visual Science. 51: 1365–1372
93. Gealy EC, Kerr BC, Young RD, Tudor D, Hayes AJ, Hughes CE, Caterson B, Quantock AJ, Ralphs JR. 2007. Differential expression of the keratan sulphate proteoglycan, keratocan, during chick corneal embryogenesis. Histochemistry and Cell Biology. 128: 551–555
94. Young RD, Gealy EC, Liles M, Caterson B, Ralphs JR, Quantock AJ. 2007. Keratan sulfate glycosaminoglycan and the association with collagen fibrils in rudimentary lamellae in the developing avian cornea. Investigative Ophthalmology & Visual Science. 48: 3083–3088
95. Zhang Y, Conrad AH, Tasheva ES, An K, Corpuz LM, Kariya Y, Suzuki K, Conrad GW. 2005. Detection and quantification of sulfated disaccharides from keratan sulfate and chondroitin/dermatan sulfate during chick corneal development by ESI-MS/MS. Investigative Ophthalmology & Visual Science. 46: 1604–1614

Figure Legends

Figure 1: An orthogonal/rotated collagen fibril pattern in the chick corneal stroma. (A) Representative en block tissue SHG imaging of collagen macrostructure in the embryonic chick corneal stroma (n=4). Through focus SHG images taken from the epithelial layer towards the endothelial layer of E17 chick corneal stroma and their corresponding FFT analysis (insets) of the collagen macrosctructure orientation. Black arrowheads denote collagen orientation in the different planes, z1-z3. Scale bar: 50μm (B) Corneal cross-sections were taken through the entire cornea including the corneal epithelium, stroma and endothelium. SHG signals were only detected when collagen fibers are aligned along the imaging plane and appear as bands in the anterior and posterior stroma. Red lines connect the collagen orientation between the en face (A) and cross-section (B) views. Note that when the collagen is oriented 45º to the image plane, there is no signal (representative plane, z2). Scale bar: 50μm

Figure 2: No angular displacement of collagen fibrils in the primary stroma. En face SHG images of the embryonic chick corneal stroma at E8 and E9. En face SHG images of E8 and E9 chick corneas taken at successive lamellar planes, progressing from the epithelium towards the endothelium. The respective FFT analyses of the collagen fibril orientation at the interface are shown (insets). Bundles of collagen fibrils which give rise to the SHG signal (arrowheads) are orthogonally arranged and show no angular displacement in the primary stroma. Images of four representative samples per embryonic stage Scale bar: 50μm

Figure 3: Development of angular displacement of collagen fibril macrostructure begins on E10. En face SHG images and respective FFT analysis of E10, E12 and E14 chick corneas taken at different depths in the corneal stroma, progressing from the epithelium towards the endothelium. At E10, collagen angular displacement (63.2 ± 3.8º) from preceding layers is first evident in the anterior corneal stroma while the orthogonal layers of collagen in the posterior stroma show no angular displacement. From E10 onwards, the orthogonal collagen layers show a gradual angular displacement at

successively more superficial levels of the corneal stroma, so that by E14 the collagen shows an angular displacement of about 155.1º ± 10. The respective FFT analyses at the interface are shown (insets). Images of four, seven and six representative samples for E10, E12 and E14, respectively. Scale bar: 50µm

Figure 4: Spatial differences in the development of angular displacement of collagen fibril macrostructure in the anterior stroma during development. 3D Directionality analysis of the stromal collagen organization with development. Collagen alignment in the developing corneal stroma was quantified by the Directionality plugin in Image J. The percentage of signal/collagen aligned at each angle from -90º to +90º within the image was evaluated and plotted against corneal stromal depth. At E9, the peaks show a preferred alignment of collagen at -90º, 0º and +90º, indicating an orthogonal/non-rotational collagen organization with respect to the choroid fissure (0º). At E10 onwards, the peaks display a shift from 0º illustrating the rotation of collagen at the anterior stroma. In the posterior stroma no shift in the peaks of the preferred collagen alignment is observed, illustrating that there is no rotation in the posterior stroma. Representative data from three samples for each embryonic stage.

Figure 5: The amount of angular displacement of collagen fibril macrostructure begins on E10 and increases with development. Cross-sectional SHG imaging of the collagen in the embryonic chick corneal stroma. Vibratome corneal sections (200-250 µm thick) taken through the center of the cornea, from successive developmental stages (E8-E14) were examined by SHG. Cross-sectional SHG imaging did not display any banded SHG signal pattern in the embryonic corneal stroma at E8 and E9, supporting the premise that the collagen layers show no angular displacement at these developmental stages. At E10, a banded SHG signal pattern becomes apparent in the anterior stroma (arrow) as a result of the rotation of the collagen in the anterior stroma. From E12 onwards, two banded SHG signal patterns are evident highlighting a greater angular displacement of the collagen at a greater level of the stromal depth. Representative images from at least three samples for each embryonic day. Scale bar: 100µm

Figure 6: Branching and anastomosing in the anterior chick corneal stroma. Representative 3D volume rendered cross-section of E18 chick cornea (n=3). Orthogonal

XY- and YZ- volume 3D reconstructions showing highly interconnected adjacent collagen layers with increased amount of branching and anastomosing (arrowheads).

Figure 7: Mechanical stimuli due to decreased IOP do not influence collagen fibril macrostructure in the corneal stroma during development. *Ex ovo* chick corneal development at E15. (A) Chick eye showing retention of tube implanted at E3 (arrow). (B) Control, opposite eye of chick with tube implanted at E3. (C) Gross size of intubated eye. (D) Gross size of control, opposite eye. (E) Manually segmented stacks of 2D FFTs showing collagen rotation in the intubated eye and (F) in the control, opposite eye. Note that the intubated eye is markedly smaller, but has the same degree of collagen rotation indicating that IOP does not affect collagen organization. Eye intubation experiments were performed three times, one dozen eggs per experiment.

Figure 8: Keratocytes with an initially random orientation acquire an orthogonal one by E9 and display angular displacement in the anterior stroma. Keratocyte organization in the embryonic chick corneal stroma was investigated by confocal microscopy. (A) Maximum intensity projections of en block datasets of the embryonic chick corneal stroma showing staining of actin (Phalloidin; green) and nuclei (Propidium Iodide; red). At E10, keratocytes fully invade the primary stroma. Arrowheads denote the epithelial basal lamina. Scale bar: 50μm (B) At E8, two dimensional, en face images show that most of the keratocytes have a random orientation in the anterior-mid stroma, but favour a parallel orientation in the posterior stroma aligned to the choroid fissure axis. At E9, keratocytes in the anterior stroma displayed a clockwise rotation (59.6 ± 7.1º) and orthogonal organization. Representative images from four samples per embryonic day and the respective FFT analyses at the interface are shown (insets). Scale bar: 50μm

Figure 9: The angular displacement of keratocytes gradually increases with development. En face confocal imaging of the keratocytes and respective keratocyte orientation FFT analysis of E12, E14 and E16 chick corneal stroma. From E9 onwards, keratocytes take up a more orthogonal organization and their angular displacement gradually increases as the cornea develops so that by E16 they display a clockwise rotation of 195.7 ± 13.6º. The respective FFT analyses at the interface are shown (insets).

All images are representative of at least four samples per embryonic stage. Scale bar: 50μm

Figure 10: Spatial differences in the angular displacement of keratocytes in the anterior stroma during development. 3D Directionality analysis of the keratocyte organization in the corneal stroma with development. Directionality analysis, representing the percentage of keratocytes aligned along a particular direction (from -90º to +90º) against corneal stromal depth. At E8, keratocytes are predominantly orientated randomly along the choroid fissure axis (0º), as shown by the appearance of various peaks. At E9, peaks appear at -90º, 0º and +90º, indicating that the cells take up a more orthogonal orientation. Also, there is a shift in the peaks from 0º in the anterior stroma illustrating rotation of the keratocytes in the anterior stroma. There is an increase in the shift of the peaks with development, indicating an increase in the keratocyte angular displacement through the anterior corneal stromal depth as the cornea develops. In the posterior stroma the keratocytes are orthogonally organized but no rotation is evident. Representative data from three samples for each embryonic day."

Figure 11: Relationship between collagen fibril macrostructure and keratocyte organization in the embryonic chick corneal stroma. Manually segmented stacks of 2D FFTs were generated (top panel) for the collagen (green) and keratocytes (red). Each spoke highlights the predominant directionality within each layer, while the chiral pattern denotes the angular displacement within the corneal stroma. The angular displacement (middle panel) and the percentage of rotated stroma over total stromal thickness (bottom panel) were calculated. At E9, keratocytes display an angular displacement of 59.6 ± 7.1º in the anterior stroma. In regards to collagen, FFT analysis did not reveal any collagen angular displacement at this developmental stage. Rotation of the collagen planes is first evident at E10 (63.2 ± 3.9º) in the anterior stroma after keratocytes have fully invaded the corneal stroma. With development there is a gradual increase in keratocyte and collagen angular displacement. Representative data from at least four samples for each embryonic day." Error bars represent SE. * Statistically significant ($p < 0.001$) when compared to the previous embryonic day. ** Statistically significant ($p < 0.001$) when compared to E10."

Figure 1

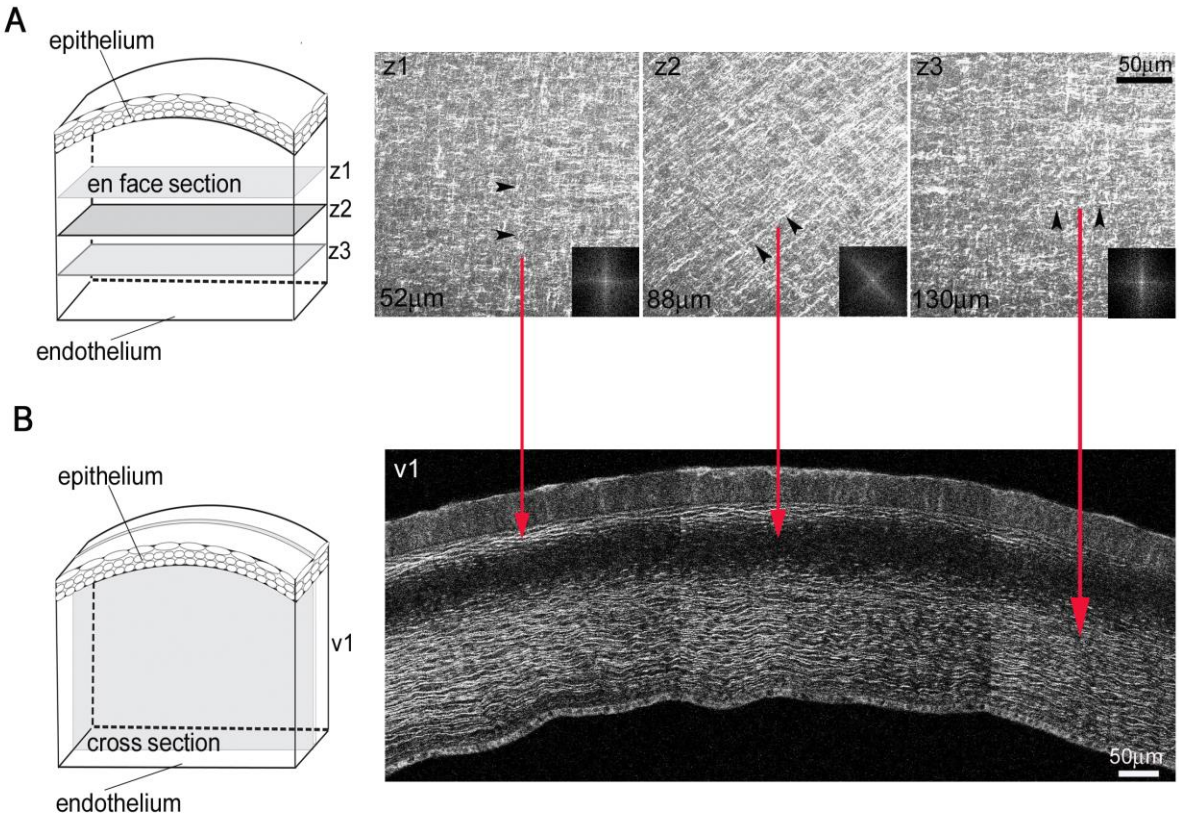
A
epithelium
en face section
z1
z2
z3
endothelium
z1
z2
z3
50µm
52µm
88µm
130µm
B
epithelium
v1
cross section
endothelium
v1
50µm

Figure 2

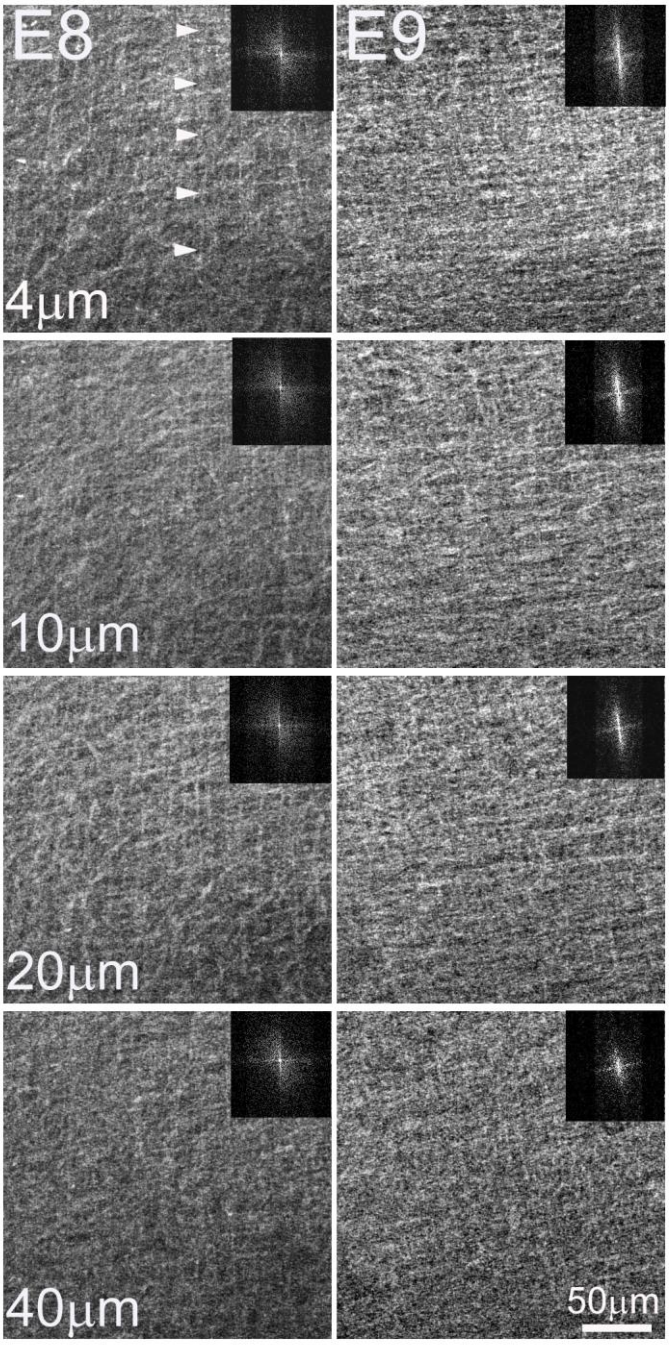

Figure 3

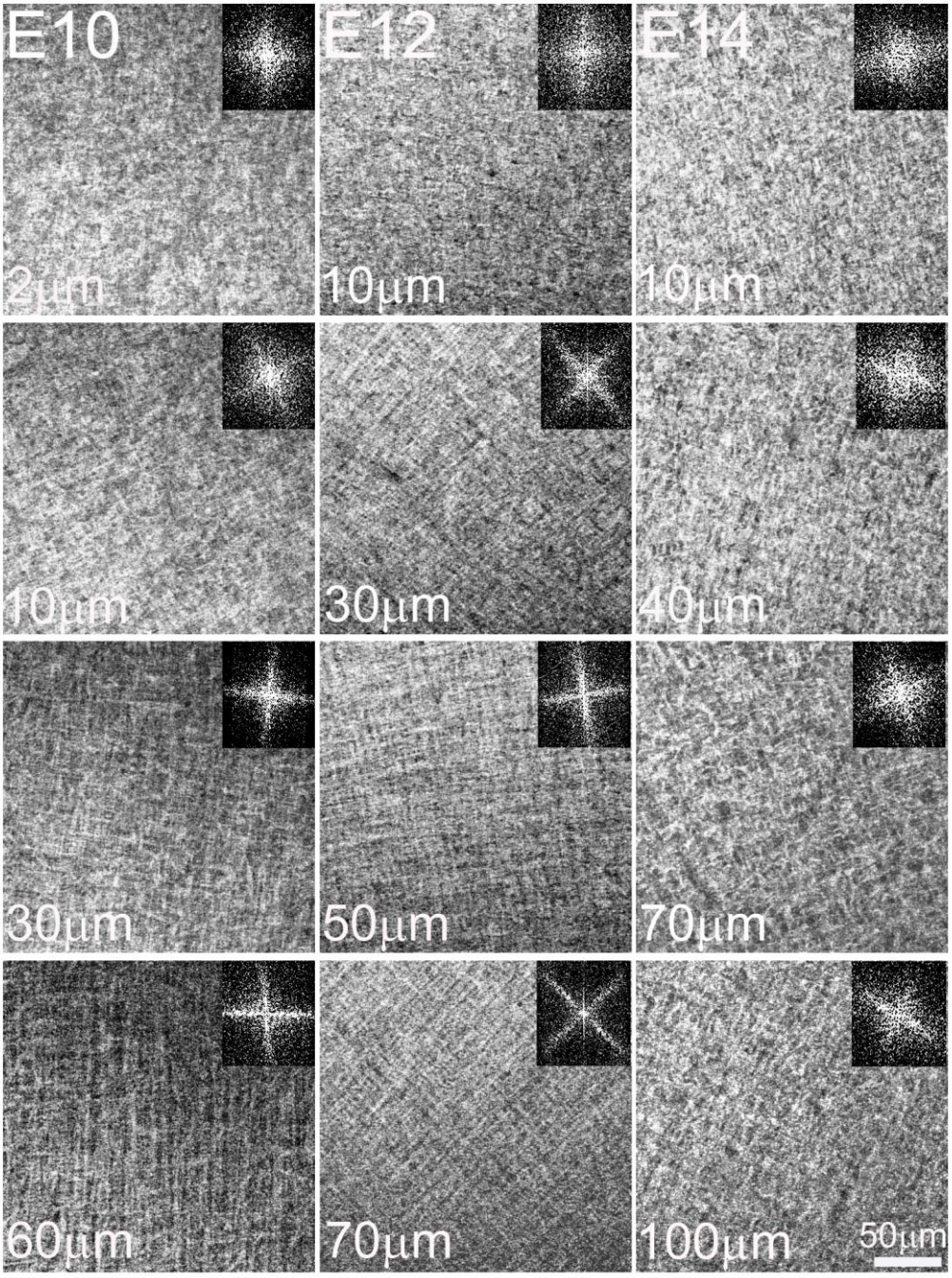
E10
E12
E14
2μm
10μm
10μm
10μm
30μm
40μm
30μm
50μm
70μm
60μm
70μm
100μm
50μm

Figure 4

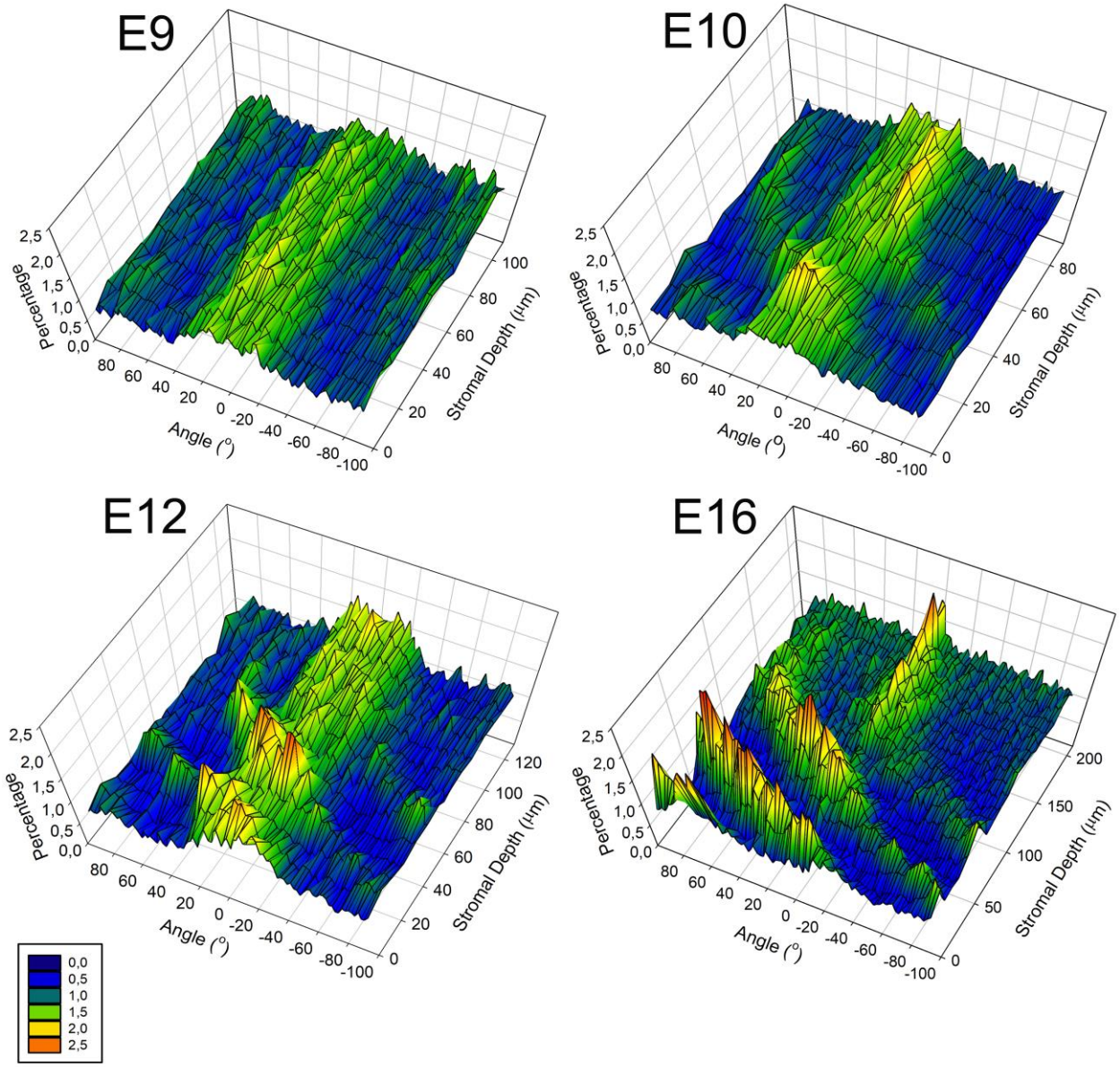
E9
E10
E12
E16
Percentage
Angle (°)
Stromal Depth (µm)
2,5
2,0
1,5
1,0
0,5
0,0
80
60
40
20
0
-20
-40
-60
-80
-100
100
120
150
200
50

Figure 5

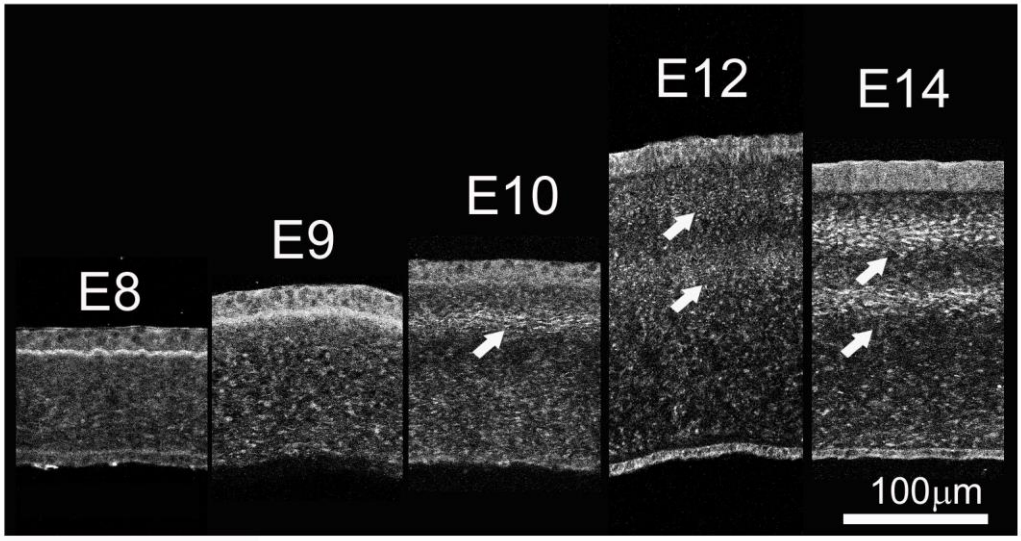

Figure 6

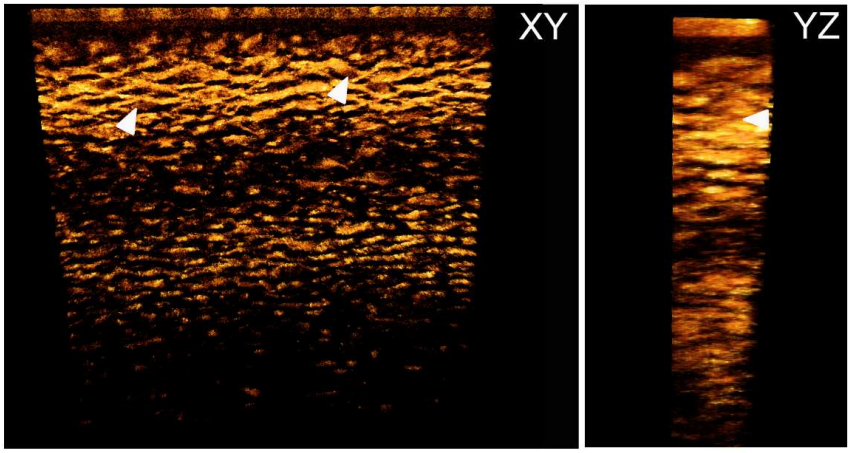

Figure 7

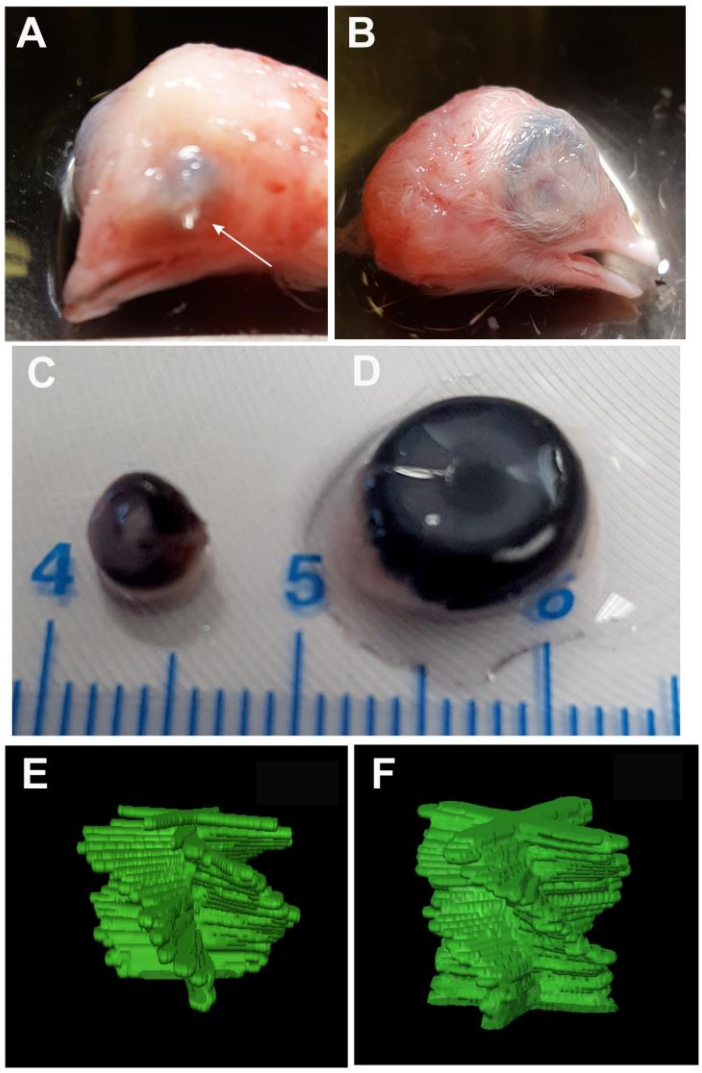

Figure 8

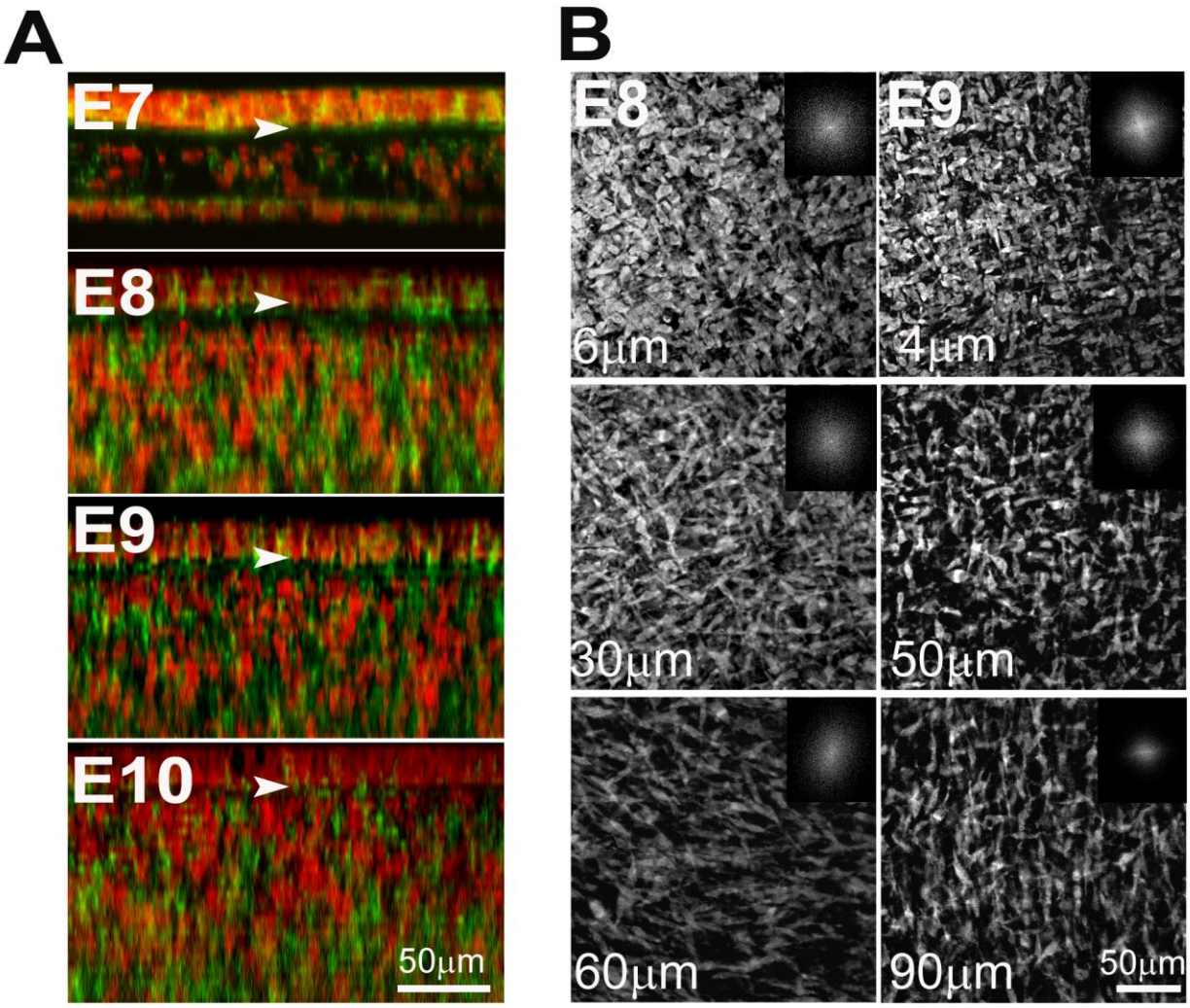

Figure 9

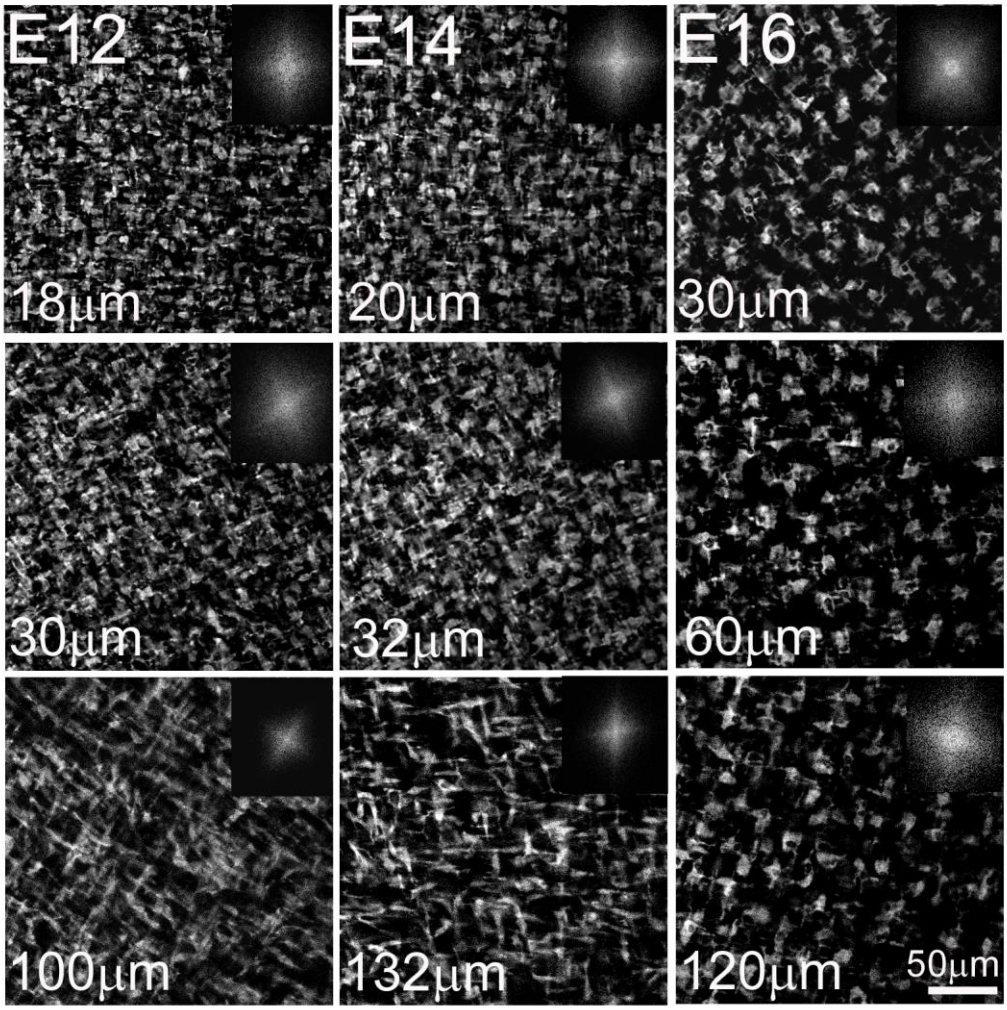
E12
18μm
E14
20μm
E16
30μm
30μm
32μm
60μm
100μm
132μm
120μm
50μm

Figure 10

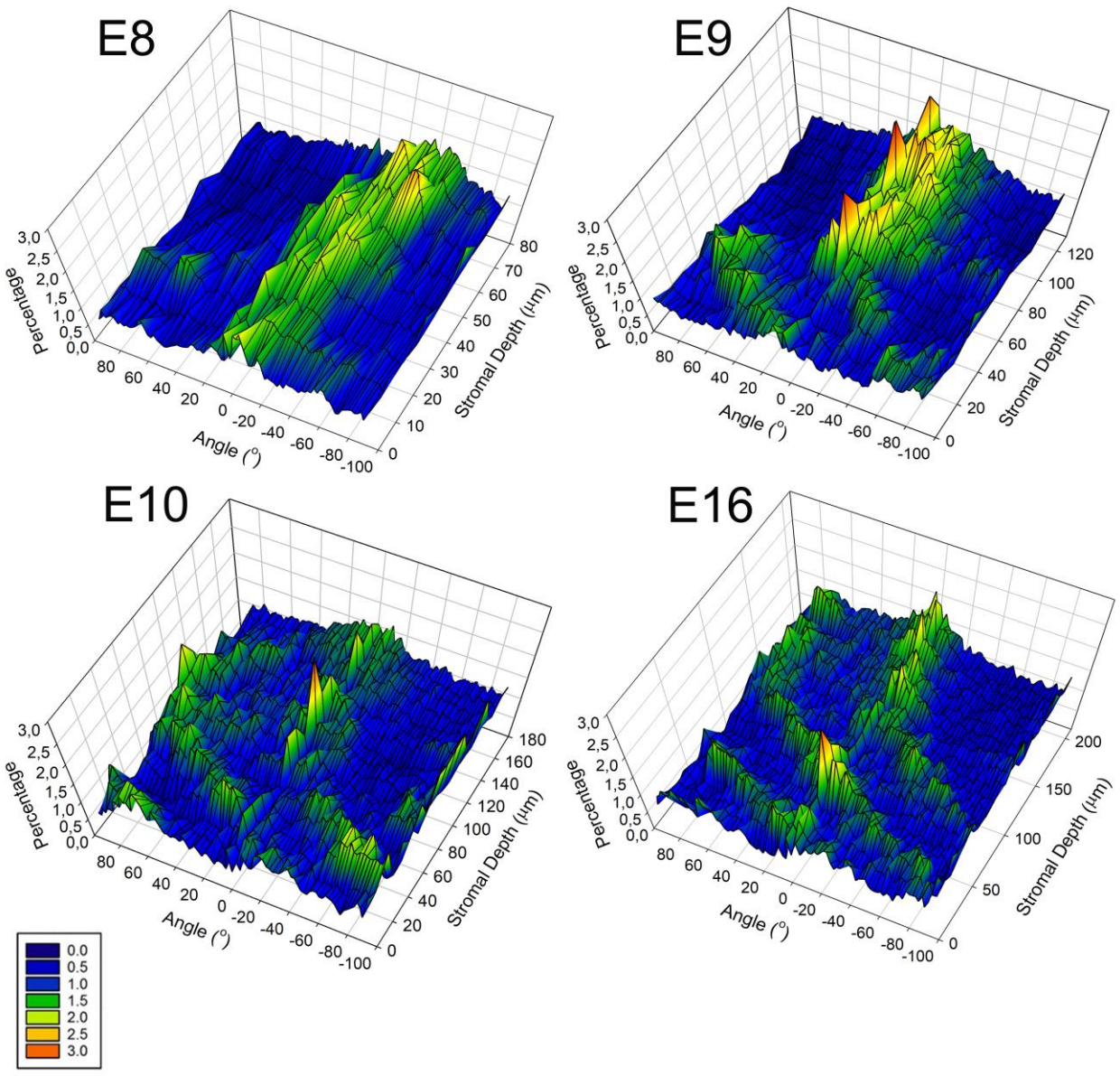
E8
E9
E10
E16
Percentage
Angle (°)
Stromal Depth (µm)
0.0
0.5
1.0
1.5
2.0
2.5
3.0

Figure 11

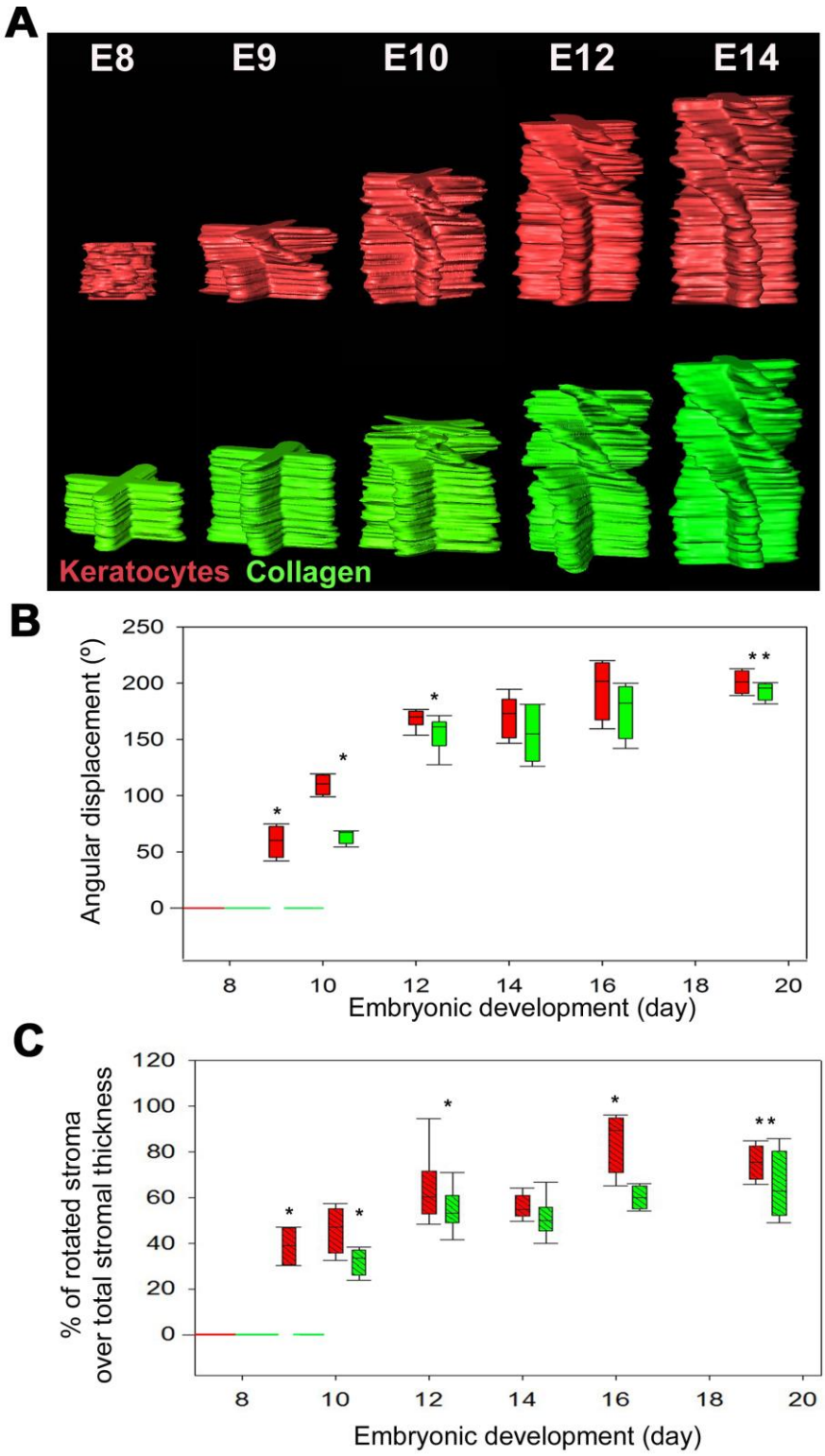
A
E8
E9
E10
E12
E14
Keratocytes
Collagen
B
Angular displacement (°)
250
200
150
100
50
0
8
10
12
14
16
18
20
Embryonic development (day)
C
% of rotated stroma over total stromal thickness
120
100
80
60
40
20
0
8
10
12
14
16
18
20
Embryonic development (day)

Table 1: The angular displacement of keratocytes and collagen in the embryonic chick corneal stroma.

Embryonic Day	Angular Displacement (±SE)		% Rotated stroma over total stromal thickness (±SE)	
	Keratocytes	Collagen	Keratocytes	Collagen
8	0	0	0	0
9	59.3 ± 7.1*	0	38.8 ± 4.5*	0
10	109.9 ± 4.5*	64.5 ± 3.9*	45.9 ± 5.2	32.2 ± 3.8*
12	168.5 ± 3.1*	155.3 ± 5.6*	64.3 ± 5.8*	55.1 ± 3.5*
14	170.6 ± 7.3	155.1 ± 10.0	56.0 ± 2.1	51.0 ± 2.2
16	195.7 ± 13.6	176.6 ± 12.5	85.0 ± 6.8*	60.1 ± 2.6
19	201.0 ± 5.2**	193.4 ± 4.1**	75.4 ± 3.9**	65.1 ± 7.6**

These are the average values obtained from at least four chick corneas per embryonic day (N=4-7). The angular displacement measurements were repeated three times.

* $P<0.001$ when compared to the previous E

** $P<0.001$ when compared to E10

Supplementary Material

Supplementary Video 1: Manually segmented stacks of 2D FFTs of collagen corneal stromal organization at E8 and E9. The reconstructed 3D rendered SHG movie of the through-focus SHG data, going from the epithelium towards the endothelium, at E8 and E9 showing the orthogonal/non-rotational collagen lamellar organization in the corneal stroma.

Supplementary Video 2: Through-focus SHG collagen dataset along with the manually segmented stack of 2D FFT at E10. The corresponding FFT (inset), as well as the manually segmented stack of the FFT dataset are also shown**.** At E10, there is an

angular displacement of collagen lamellae in the anterior stroma, while in the posterior stroma there is an orthogonal/non-rotational organization.

Supplementary Video 3: Through-focus SHG collagen dataset along with the manually segmented stack of 2D FFT at E12. The corresponding FFT (inset), as well as the manually segmented stack of 2D FFT dataset are also shown. As the cornea develops, there is an increase in the angular displacement of collagen lamellae in the anterior stroma, but the posterior stroma does not show any angular displacement/rotation.

Supplementary Video 4: Keratocyte organization in the embryonic chick cornea along with the manually segmented stack of 2D FFT at E8. Through-focus dataset of the keratocyte organization in the embryonic chick corneal stroma, going from the epithelium towards the endothelium. The corresponding FFT, as well as the manually segmented stack of 2D FFT dataset are also shown. At E8, most cells appeared to be randomly oriented within the anterior-mid stroma, while cells in the posterior stroma showed a preferential parallel orientation aligned with the choroid fissure.

Supplementary Video 5: Keratocyte organization in the embryonic chick cornea along with the manually segmented stack of 2D FFT at E9. Keratocyte en face dataset and the corresponding FFT dataset along with the manually segmented stack of 2D FFT at E9. On E9, keratocytes developed an orthogonal orientation and displayed an angular displacement in the anterior stroma**.**

Supplementary Video 6: Keratocyte organization in the embryonic chick cornea along with the manually segmented stack of 2D FFT at E12. Keratocyte en face dataset and the corresponding FFT dataset along with the **manually segmented stack of 2D FFT** at E12. With development, the angular displacement of keratocytes increases.